



**International Journal of Information and Communication Technology**

ISSN online: 1741-8070 - ISSN print: 1466-6642

<https://www.inderscience.com/ijict>

---

**Mathematical modelling of multi-UAV scenario planning based on 3D LiDAR**

Ruishuai Chai

**DOI:** [10.1504/IJICT.2024.10063064](https://doi.org/10.1504/IJICT.2024.10063064)

**Article History:**

Received:	07 November 2023
Last revised:	08 January 2024
Accepted:	11 January 2024
Published online:	12 May 2024

---

# Mathematical modelling of multi-UAV scenario planning based on 3D LiDAR

---

Ruishuai Chai

Henan Industry and Trade Vocational College,  
Zhengzhou 450046, China  
Email: hnchairuishuai@163.com

**Abstract:** In order to improve the operation efficiency of multi-UAV groups, this paper studies the mathematical modelling of multi-UAV scene planning, takes 3D LiDAR technology as the base navigation technology, and uses the bacterial foraging algorithm as the multi-objective optimisation algorithm. Moreover, this paper appropriately improves the defects of the algorithm, and introduces the bacterial population in the algorithm into the log-linear model to improve the two basic behaviours of the algorithm, the trend and the migration, so that the local search of the algorithm is more accurate. In addition, this paper introduces Gauss-Cauchy variation to ensure the diversity of bacterial populations and ensure that the algorithm results are close to the global optimal value. Through experimental research, it is known that the algorithm proposed in this paper can drive the drone to conform to the flight trajectory as a whole, achieve the expected fusion positioning accuracy, and meet the requirements of autonomous cruising. The average registration time is 120 milliseconds, which meets the real-time perception of the scene and pose estimation requirements during cruising. The experimental study shows that the multi-UAV scene planning method based on 3D LiDAR can effectively improve the optimal control effect of multi-UAV.

**Keywords:** 3D LiDAR; multi-UAV; scene planning; mathematical modelling.

**Reference** to this paper should be made as follows: Chai, R. (2024) 'Mathematical modelling of multi-UAV scenario planning based on 3D LiDAR', *Int. J. Information and Communication Technology*, Vol. 24, No. 6, pp.1–22.

**Biographical notes:** Ruishuai Chai studied in Henan normal University from 2000 to 2004 and received his Bachelor's degree in 2004. From 2007 to 2009, he studied in Huazhong University of Science and Technology and received his Master's degree in 2009. Currently, he works in Henan Industry and Trade Vocational College. He has published ten papers. His research interests are mathematics education and student work.

---

## 1 Introduction

Generally discussed LiDAR is 3D imaging LiDAR. According to the different carrying platforms, it can be divided into spaceborne, airborne and ground-side. The spaceborne LiDAR mainly relies on satellite platforms, so it has a high orbit and can basically measure every corner of the Earth (Hongming et al., 2022). The airborne LiDAR is

mainly carried on the aircraft to collect large-scale point cloud data. Ground-side LiDAR is mainly used in the field of unmanned driving and surveying and mapping, and can be mounted on a car or fixed on a tripod. The data collected by LiDAR is in the form of a point cloud, which presents the scanning results of objects in the form of points, and each point contains three-dimensional information, generally including the reflection intensity and reflectivity of the object (Zohdi, 2020). Among them, unmanned aerial vehicle LiDAR (UAV LiDAR) is attracting the attention of researchers and engineers due to its low cost, convenient data collection and large measurement scene (Batinovic et al., 2021).

Integrate LiDAR, inertial measurement unit/global position system (IMU/GPS) and other instruments on the same UAV platform. After setting the communication mode between instruments and the control mode of the instrument, if you directly collect data, although it can be collected The data is obtained, but there are many problems with the data at this time: first, the coordinate information of the measured data is inaccurate, and even the data collected multiple times for the same feature scene will be different. These errors are mainly caused by the installation of each instrument. The difference between the position and the IMU/GPS will also cause errors such as the tilt and jitter of the aircraft's attitude during the acquisition process, the changes of the satellites connected to the IMU/GPS on the aircraft, and each time the instrument is removed and reinstalled. Slight changes in position, etc. (Miao et al., 2020); secondly, for multi-sensor platforms, instruments may also influence each other. If there are multiple active remote sensors, the energy emitted by them may interfere with each other, or the energy emitted by active remote sensors may interfere with each other. It will be accepted by passive remote sensors and cause data errors (Wang et al., 2020); then the surrounding environment and ground objects in the acquisition process will also affect the generated data, such as sunlight noise, ambient light noise, bird flocks, and ground objects. Too dense or too sparse (Tang et al., 2018); finally, for a large feature scene, a single flight cannot complete the collection task, so it is necessary to consider how to design the route to ensure that the data collected multiple times can be well matched. In general, scientific research and engineering personnel currently need a set of reliable and effective UAV LiDAR system integration, data processing and acquisition solutions to ensure that the final data obtained has good quality (Petrlik et al., 2020).

Comparing the UAV with the manned aircraft, it is found that the advantages of the UAV are reflected in its lighter weight and smaller size (Quan et al., 2020). There is no need to consider safety issues such as cockpit, environmental control, and ejection life-saving when constructing UAVs, and the tasks performed by UAVs are more single than that of manned aircraft (Le et al., 2019). Therefore, when UAVs fly and complete tasks more flexibility. Usually the mass of UAVs is between tens of grams and hundreds of kilograms. Some UAVs for strategic reconnaissance missions and ground attack missions are slightly higher in mass than other types of UAVs, and have better survivability on the battlefield. Because there is no need to take into account the physiological problems of the pilot, the manoeuvrability of the UAV has been improved to a certain extent, and the difficult manoeuvring work that the pilot cannot complete can be realised (Choi et al., 2020). The stealth design of the drone body makes it less difficult to perform tasks in different environments. The investment cost of UAV is low, and the investment cost in launch, recovery, use, maintenance, etc. is lower, and its dependence on the airport runway is small, and the difficulty of manoeuvring deployment is lower. When the drone is flying, the operator must use the ground control method to formulate

the flight plan and plan the flight route, and then send the relevant data to the onboard control system of the drone, and the onboard control system will complete the corresponding flight according to the set data task (Baca et al., 2021). In addition, the ground controller can directly control and operate the UAV from the ground control station according to the actual needs, which is similar to various air flight operations on the ground (Qin et al., 2019).

UAV technology has been continuously improved and perfected in recent years, and the advantages that can be obtained in war have become more and more obvious. It has developed into an important military research and development project in many countries. With the global research boom in the field of UAVs, information warfare is becoming more and more fiercer, and the complexity of the confrontation environment is further enhanced. The future research of UAVs will mainly focus on formulating UAV mission plans, mastering UAV autonomous flight technology and the trajectory planning of the UAV is carried out in directions such as (Choi et al., 2021). As an important part of the development of aviation technology, air force combat capability and modern national defence construction, my country is currently conducting in-depth research on the integrated autonomous control and reconnaissance UAV combat platform system based on ground control station commands, and then based on this platform to achieve rapid combat and target of accurate combat. The UAV's mission planning, autonomous flight technology, flight control technology, and planning routes play a decisive role in whether it can fully exert its combat capability (Krátký et al., 2021).

Zhou et al. (2020) analyses the problem of jamming planning for shore-based warning radars when two UAVs are covering the penetrating aircraft group, which includes the routes under the lateral jamming and forward and backward jamming conditions respectively formulated before the jamming UAV performs the task. The planning method realises the purpose of covering the penetration fighter from a certain angle and generating an effective interference sector in this direction, and finally obtains the interference flight path in various environments. Şmuleac et al. (2019) proposed and established a UAV interference early warning radar model. When solving the optimal path of a single UAV, the calculation was performed according to the angular velocity of the penetration aircraft and the UAV relative to the early warning radar and other constraints. The obtained simulation the data shows that this method realises cover through the speed of the drone, which greatly saves the resources of the drone. Ulku et al. (2019) quantitatively studies the false targets in the pitch and azimuth planes based on the cover channel to deceive and interfere with the coordinated operation of the UAV swarm airspace, and discuss the corresponding air deployment method, which provides an example for the actual operation of the UAV swarm to cover the penetration of air power. important basis. Petráček et al. (2021) established a mathematical model for optimising the radar track of multi-machine jamming networking. The simulation results show that the success probability of jamming of the false target track planned by this model can be improved, and the interference can be minimised at the same time thrust during flight. Basiri et al. (2022) established a distributed optimisation UAV jamming trajectory mathematical model. The difficulty of collaborative jamming is reduced under this planning model, so that false targets can avoid the threat area and directly reach the target area.

The rapid development of information technology and the wide application of UAVs have made modern flight tasks gradually develop in the direction of more difficult

execution and faster flight speed, which puts forward higher requirements and challenges for trajectory planning. The current trajectory planning has problems such as huge planning space, complex and dynamic task environment, and a variety of strong coupling constraints. In terms of the overall research level at home and abroad, it is difficult to establish a model for the trajectory planning problem. In theory, there is no algorithm that has strong applicability and can solve all problems. Researchers have conducted extensive and in-depth research on planning algorithms, and are currently working to find an algorithm that plans better and takes less time. In mountainous areas with high mountains and steep slopes and surrounded by clouds and fog, high-resolution remote sensing satellites are greatly affected when acquiring images. In terms of acquiring agricultural production and application information and communications, technical research is far from mature, and there is no Human-machine has many inherent advantages in plant protection applications. Compared with traditional mechanical plant protection equipment, UAVs can operate in a larger area in a single day, have strong adaptability, and are easy to promote (Selecký et al., 2019).

At present, there are various UAV trajectory planning algorithms, among which there are many two-dimensional or 2.5-dimensional trajectory planning methods, and the methods are also relatively mature. Due to the closer proximity of three-dimensional space to the practical application environment of UAVs, many scholars and experts have gradually shifted their focus to three-dimensional trajectory planning and proposed many improved algorithms. For the three-dimensional global static trajectory planning problem, it is currently possible to quickly generate trajectories under simple threats, but there is a lack of consideration for the optimal trajectory under complex environmental constraints, and it is not possible to simultaneously consider both complex environmental constraints and drone performance constraints and characteristics for optimal trajectory planning. For the three-dimensional dynamic trajectory planning problem, there is currently less research, and the sudden threats considered are all single and simple circular threats. Simplifying the three-dimensional environment to the minimum threat surface is essentially a two-dimensional environment, and the accuracy of the planned trajectory is not enough. In the context of the booming development of spatial information technology and the increasingly widespread application of drones, this poses greater challenges and requirements for the three-dimensional trajectory planning of drones, and these issues need to be resolved as soon as possible.

The innovation of this paper lies in the analysis and optimisation of UAV 3D LiDAR scene scheduling based on bacteria foraging algorithm. According to the specific scene situation on the UAV route, the scheduling model is set with a variety of constraints in line with real life and in-depth analysis. Then the mathematical model is combined with the NBFA algorithm in this paper, and the evaluation standard of scheduling scheme is established. The optimal solutions of each algorithm are obtained through simulation experiments, and then the advantages of NBFA algorithm in dealing with scheduling problems are obtained by comparing the optimal solutions of each algorithm.

The goal of this article is to study the design and implementation of enhanced synthetic visual schemes for UAVs in different stages of three-dimensional perception, understanding, and decision-making in complex environments. Design and validate an enhanced synthetic visual scheme for situational awareness in complex environments using visual simulation technology.

The organisational structure of this article is as follows: describe the background and significance through the introduction, introduce the research content of this article,

improve the algorithm, make the local search of the algorithm more accurate, and ensure that the algorithm results are close to the global optimal value; perform mathematical modelling for multi-drone scene planning based on 3D LiDAR create a 3D point cloud map and set the target points we want to go to in the 3D point cloud map; verify the effectiveness of the algorithm model through experiments, and provide research conclusions and prospects for this article.

This paper studies the mathematical modelling of multi-UAV scene planning, and uses 3D LiDAR as the basis to verify the model effect through intelligent simulation, which provides a reference for subsequent UAV scene planning.

## **2 Multi-UAV group planning algorithm**

Improve the informatisation degree and work efficiency of UAV, and ensure the normal operation of UAV group. The early construction and later operation and maintenance of the UAV dispatching system can not be separated from the technical support of software and hardware. The UAV working online, the information flow during the operation period, and the line equipment conditions can be accurately collected, transmitted, and comprehensively processed.

Communication system is a very important and complex system in urban UAV scene planning. It can establish a real-time audio-visual information link network to ensure accurate transmission of all kinds of information. The communication system is composed of closed-circuit television system, dispatching telephone system, wireless dispatching system, clock system, broadcasting system, communication power supply system, etc.

In contemporary society, there are a large number of production problems that need mathematical functions to solve. However, with the increase of the complexity and the expansion of the number of problems, those traditional mathematical methods are no longer suitable. Therefore, a large number of researchers have created ant colony algorithm, neural network, Tabu search and other intelligent algorithms based on the biological behaviour of nature. These intelligent algorithms have many advantages over traditional mathematical methods in solving complex abstract problems. However, due to the setting of coefficients, these algorithms are prone to fall into local optimal results and cannot achieve the optimal results that people expect.

The main work of this paper is to study the theory and application on the basis of the basic bacterial foraging algorithm, improve the algorithm according to the defects of the algorithm, and combine the actual needs of three-dimensional LiDAR detection, so a Gauss Cauchy adaptive bacterial foraging algorithm based on log-linear model is proposed. Based on the actual UAV scene planning work plan, the mathematical model of scheduling optimisation that conforms to the actual operation of UAV scene planning is rebuilt, and then the improved algorithm is combined with the rebuilt mathematical model of scheduling optimisation to improve the effect of UAV scene planning.

### *2.1 Basic operation of bacterial foraging algorithm*

The UAV scheduling problem can be described as follows: given the location of the scheduling centre and the location of each task point to be executed, the UAV needs to be

arranged to execute tasks from the scheduling centre to each task point. In the scheduling scheme, each task point can only be executed by one UAV, and each UAV can execute multiple task points, but the flight distance of each UAV cannot exceed its maximum flight distance limit. In addition, priority and time window constraints of each task point, mountain terrain, no fly zone and other threat factors need to be considered during flight. The ultimate optimisation goal is to maximise the total benefits of the scheduling scheme, the cost is minimal.

When solving the multi-objective optimisation problem of the UAV group, the calculation process of the bacterial foraging algorithm (BFA) algorithm imitates the three basic operations of *Escherichia coli*. That is, an algorithm operation cycle includes a chemotaxis operation, a reproduction operation, a elimination and dispersal operation, and finally the algorithm operation ends and outputs the result. The BFA algorithm first regards each bacterial individual as the optimal solution of the problem (the location information of the bacteria represents the candidate optimal solution of the algorithm), and initialises each bacterial individual. After that, it finds the optimal solution of the multi-objective problem in the global scope through iterative calculation.

The introduction of letter symbols is to better represent all kinds of information of the algorithm:  $j, k, l$  represent the number of chemotaxis operation, reproduction operation, elimination and dispersal operation that have occurred in the bacterial foraging algorithm, respectively;  $D$  represents the searchable dimension of bacteria in the entire living space, and  $S$  represents the population number of bacteria in the entire environment;  $N_c$  represents the maximum number of iterations of the bacteria chemotaxis operation;  $N_s$  represents the maximum number of steps the bacteria can move in a random direction;  $N_{re}$  represents the maximum number of iterations the bacteria allow replication to occur;  $N_{ed}$  represents the maximum number of iterations that bacteria can perform elimination and dispersal operations,  $P_{ed}$  represents the probability of bacteria dispersal in any direction in all random directions;  $C(i)$  represents the adaptive search step size of bacteria.

$P(j, k, l) = \{\theta^i(j, k, l) | i = 1, 2, \dots, s\}$  represents the position of the individual in the population after the  $j^{\text{th}}$  chemotaxis operation, the  $k^{\text{th}}$  reproduction operation and the first elimination and dispersal operation.  $J(i, j, k, l)$  represents the fitness function value of bacteria  $i$  after the  $j^{\text{th}}$  chemotaxis operation, the  $k^{\text{th}}$  reproduction operation and the first elimination and dispersal operation.

A bacterium picks a random direction at a certain location and moves forward. If the fitness value of the region is lower than that of the previous region, the bacteria will rely on the rotation of the flagella to randomly select a forward direction again. If the fitness value of bacteria in any area is higher than the fitness value of the previous area, the bacteria will not change direction and continue to dispersal until it encounters a poor food environment, after which it will change its direction again.

$$\theta^i(j+1, k, l) = \theta^i(j, k, l) + C(i)\varphi(i) \quad (1)$$

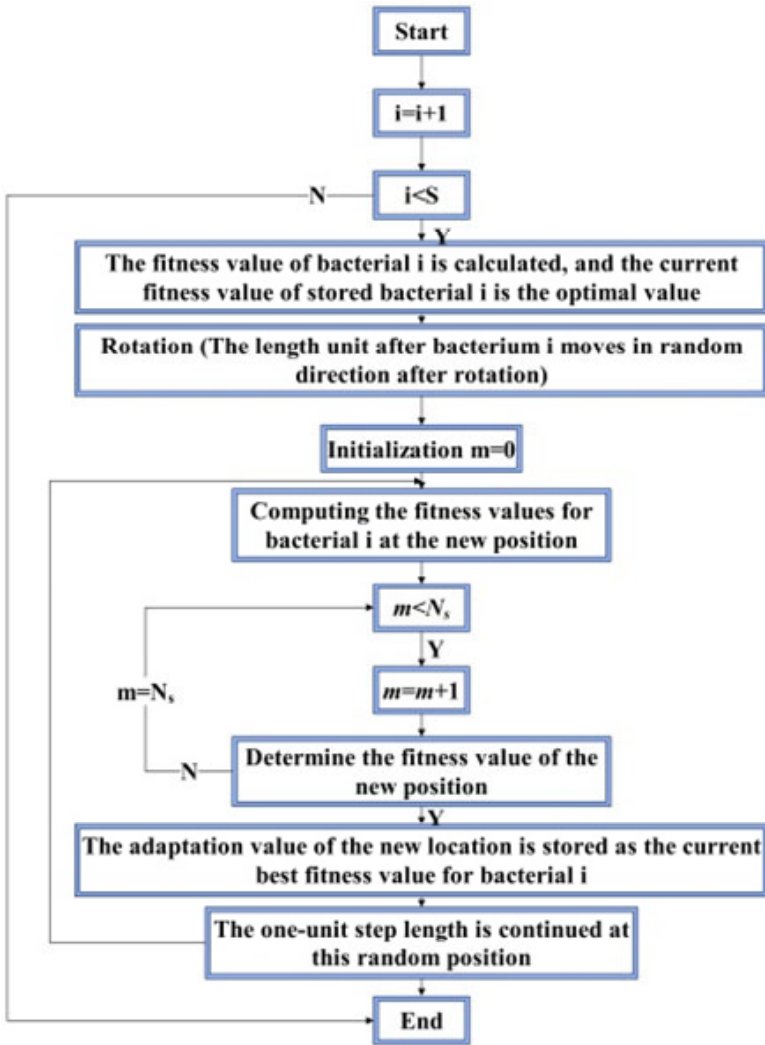
$$\varphi(i) = \frac{\Delta(i)}{\sqrt{\Delta(i)^\Gamma \Delta(i)}} \quad (2)$$

A bacterial population is  $S$ , the location of a bacterium represents a candidate solution to the problem, and the information of bacterium  $i$  is represented by a  $D$ -dimensional vector  $\theta^i = [\theta_1^i, \theta_2^i, \dots, \theta_D^i]$ ,  $i = 1, 2, \dots, S$ , where  $\theta^{i(j+1, k, l)}$  in formula (1) represents each step

of the chemotaxis operation of bacterium  $i$ .  $C(i)$  represents the step length of forward search for seedling  $i$  when it is fed, that is, the adaptive step length of bacteria. In formula (2),  $\varphi(i)$  is the angle formed by the bacteria  $i$  after changing its direction and the original advancing direction, and  $\Delta(i)$  is the unit vector after randomly changing the advancing direction.

The chemotaxis operation process is shown in Figure 1.

**Figure 1** Flowchart of chemotaxis operation (see online version for colours)

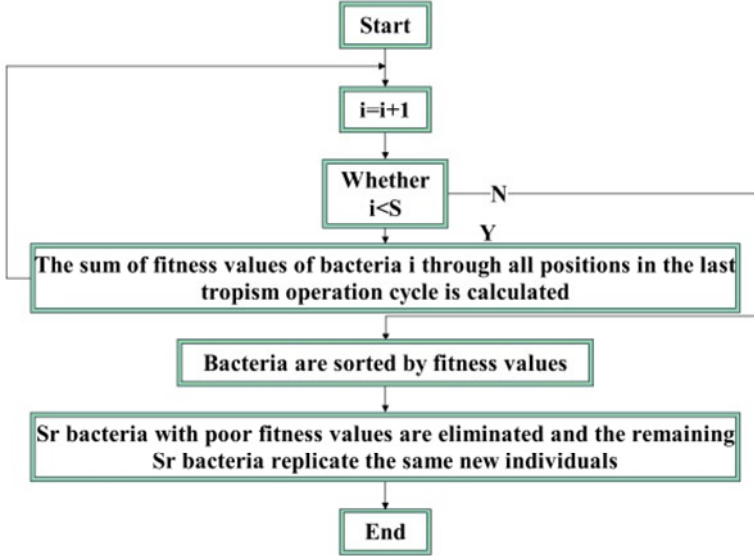


The core operation of BFO algorithm is chemotaxis operation, which has excellent local optimisation ability and affects the search ability and depth of individual bacteria, so it is a key part of BFO algorithm optimisation.

Organisms follow the natural law of survival of the fittest. When the biological environment is superior, the biological reproduction capacity is enhanced, and the

population increases; when the living environment is destroyed, the biological population decreases. Faced with the above situation, the less viable *E. coli* colonies will be eliminated by the environment, while the more foraging individuals in the bacterial population will survive and replicate themselves. In this way, the number of bacterial populations can be kept unchanged, which can ensure the global optimisation of the algorithm. The process of reproduction operation is shown in Figure 2.

**Figure 2** Flowchart of reproduction operation (see online version for colours)



$J_{health}^i$  represents the health information of bacterial individual  $i$ , which is usually expressed by the concentration of food around bacterial individual  $i$ . The higher the food concentration around the individual bacteria, the healthier the bacteria, and the stronger the ability of bacteria to eat at this moment, and vice versa. Through the above ideas, firstly, the bacterial populations in the whole environment are sorted according to the size of the health degree, and then the median value of the health degree of the bacterial population is selected. Next, the bacterial population  $S_r$  whose health value is less than the intermediate value is eliminated ( $S_r = S/2$ , where  $S$  represents the total number of bacteria before elimination). Finally, the remaining half of the bacteria  $S_r$  (the half of the seedlings with a health value greater than or equal to the median value) are replicated. Moreover, the post-replication bacteria and the pre-replication bacteria with a health degree greater than or equal to the median value have the same feeding ability and the same health degree. Through the reproduction operation, the bacterial population will not change under any conditions, which can ensure that the candidate feasible solutions of the algorithm remain unchanged, and can also improve the computational efficiency and optimisation accuracy of the algorithm. The following formula (3) represents the health degree of any bacterial individual  $i$ :

$$J_{health}^i = \sum_{j=1}^{N_c} J(i, j, k, l) \quad (3)$$

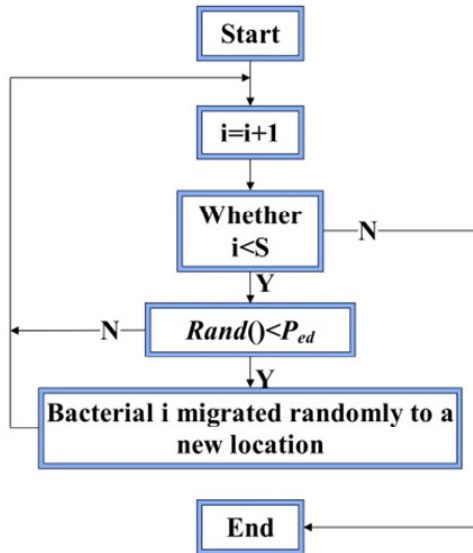
Although the above reproduction operation can ensure that the feeding ability of the offspring and the parent bacteria is exactly the same, it will replicate the bacteria with poor feeding ability in the top 50% of the bacterial health value. As a result, this strategy fails to retain the best-fit bacteria for the next generation. Therefore, the distribution estimation algorithm can be embedded in the reproduction operation. Estimation of distribution algorithm EDA (Estimation of distribution algorithm) is a random search algorithm based on the probability distribution of variables. It establishes a corresponding probability distribution model by sampling excellent individuals and analysing the statistical distribution of space, and generates the next generation of individuals based on this probability model, and iterates repeatedly to realise the evolution of the group. The specific steps are as follows:

- Step 1 After a complete trend cycle, the algorithm sorts each bacteria according to the energy (accumulated sum of fitness values).
- Step 2 The algorithm eliminates half of the bacteria with poor energy, and estimates and regenerates the half of the bacteria with better energy. If each dimension of the variable to be optimised is independent of each other, and each dimension obeys a Gaussian distribution, the bacteria are replicated according to formulas (4) and (5).

$$X_{\mu,\sigma} = r_{norm} * \sigma + \mu \tag{4}$$

$$r_{norm} = \sqrt{-2 \ln r_1} * \sin(2\pi r_2) \tag{5}$$

**Figure 3** Flowchart of elimination and dispersal operation (see online version for colours)



Among them,  $r_1$  and  $r_2$  are uniformly distributed random numbers in the interval  $[0, 1]$ ,  $\mu$ ,  $\sigma$  are the fractal mean and standard deviation vector of the optimal location of bacteria, respectively, and the product is dot product.

When the bacteria perform  $k$  times of reproduction operation, the probability of dispersal behaviour of all bacteria in the large environment is  $P_{ed}$ . At this time, all the individual seedlings will automatically generate a random number  $\text{rand}()$ . When the random number of the seedlings is less than the probability of dispersal ( $\text{rand}() < P_{ed}$ ), the bacteria will automatically die. At the same time, a new individual is randomly generated at any position in the area where the bacteria can survive to replace the bacteria that died because the random number is less than the probability  $P_{ed}$  of dispersal occurrence. However, the feeding ability and location information of the new bacteria will be different from the original bacteria. The elimination and dispersal operation can not only ensure the diversity and reliability of the bacterial population, but also make the new bacterial individuals closer to the global optimal solution, which can avoid the algorithm from falling into the local optimal solution. The process of elimination and dispersal operation is shown in Figure 3.

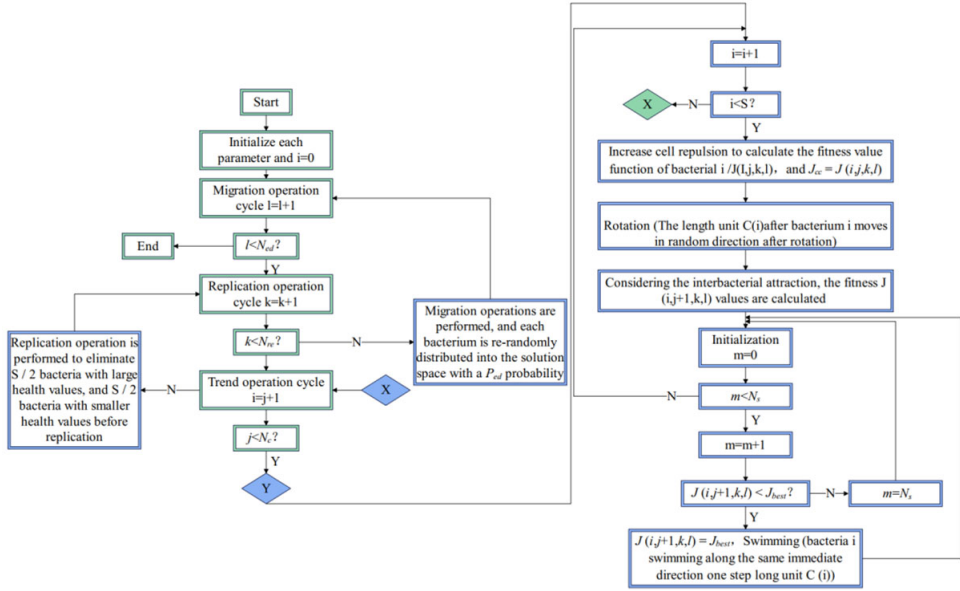
## 2.2 *Problem solving process and workflow of bacterial foraging algorithm*

In the BFO algorithm, the algorithm model first encodes bacteria for specific problems, and defines the evaluation function (fitness function) of the problem solution to be optimised and the energy state of bacteria in the solution space. The solution process for specific problems is as follows: initialise the initial generation of solution population (bacterial population), calculate the fitness function value of all individuals in the population, and then use the bacterial population sensing mechanism to iterate through the three main operators of the algorithm: chemotaxis, reproduction and migration, and finally generate the optimal solution or quasi optimal solution. The algorithm is composed of three nested loops consisting of three operations: chemotaxis, reproduction, and migration. The inner layer is chemotaxis, the middle layer is reproduction, and the outer layer is migration.

The specific process of the BFA algorithm to solve the multi-objective optimisation problem is as follows:

- 1 First, we describe and study the actual problem to be solved in detail, and understands the independent and dependent variables of the problem, constraints, and the purpose of solving the problem. Then, we determine a mathematical model that is reasonable and can solve the multi-objective optimisation problem according to the above content.
- 2 The established mathematical model formulates the coding scheme according to the BFA algorithm, so as to determine the final multi-objective optimisation function. Then, the multi-objective optimisation function and the constraints are fused with each other and converted into a fitness function.
- 3 We conduct an in-depth analysis of the three behaviours of the BFA algorithm, and determine the values of the parameters in the algorithm according to the actual problem, and then run the BFA algorithm to solve the fitness function value.
- 4 If the final number of elimination and dispersal operations of the BFA algorithm is greater than or equal to the set number of elimination and dispersal operations, the BFA algorithm stops the operation and outputs the final calculation result.

Figure 4 visually represents the workflow of the bacterial foraging algorithm.

**Figure 4** Flowchart of the BFA algorithm (see online version for colours)


### 2.3 Analysing the parameters of a bacterial foraging algorithm

When we solve multi-objective problems, we should first understand the role of various parameters in the BFA algorithm. The reason is that the parameter setting has a direct impact on the optimisation accuracy and convergence efficiency of the algorithm. The following is a detailed analysis of various parameters of the BFA algorithm.

When the bacteria live in a suitable environment (high food concentration, mild temperature, acid-base balance, etc.), the bacteria will multiply to maintain the population. Therefore, the value of the parameter  $N_{re}$  in the reproduction operation will affect the feeding ability of bacteria leaving the low food concentration area. When the maximum allowable number of chemotaxis operations for bacteria  $N_c$  is constant, if the value of the number  $N_{re}$  allowed to perform reproduction operations for bacteria is set larger, it will prolong the algorithm cycle and increase the workload of the algorithm. On the contrary, the same is true. If the value  $N_{re}$  of the maximum reproduction operation times of bacteria is set too small, although the operation cycle and complexity of the algorithm will be reduced, the algorithm will be too premature and the optimisation result will be close to the local limit value. It eventually destroys the optimisation accuracy of the bacteria feeding algorithm.

When the value of the termination condition  $N_{ed}$  of the algorithm elimination and dispersal operation (the maximum number of iterations allowed by the elimination and dispersal operation) is set to a small value, although the operation efficiency of the algorithm is increased, the result obtained by the algorithm will not be the global optimal value due to insufficient operation degree. However, if the value of parameter  $N_{ed}$  is too large, the advantage is to increase the diversity of feasible solutions of the algorithm, prevent premature maturity, and make it easier for the algorithm to find the optimal solution. The disadvantage is that the larger the value of  $N_{ed}$  is, the greater the

computational complexity of the algorithm and the more time-consuming computation. Therefore, to sum up, the reasonable choice of the dispersal probability  $P_{ed}$  is the key factor to avoid the algorithm falling into the extreme value. If the value of dispersal probability  $P_{ed}$  in the bacterial foraging algorithm is set too large, it will increase the randomness of bacteria in the optimisation process, and ultimately reduce the convergence of the algorithm and the ability to find the optimal solution.

$J(i, j, k, l)$  represents the fitness value of bacteria  $i$  in the  $j^{\text{th}}$  chemotaxis operation, the  $k^{\text{th}}$  reproduction operation and the first elimination and dispersal operation, and the influence value of the signal transmitted between the populations is shown in the following formula (6):

$$\begin{aligned} J_{cc}(\theta, P(j, k, l)) &= \sum_{i=1}^S J_{cc}(\theta, \theta^i(j, k, l)) \\ &= \sum_{i=1}^S \left[ -d_{attractant} \exp\left(-w_{attractant} \sum_{m=1}^D (\theta_m - \theta_m^i)^2\right) \right] \\ &\quad + \sum_{i=1}^S \left[ h_{repellant} \exp\left(-w_{repellant} \sum_{m=1}^D (\theta_m - \theta_m^i)^2\right) \right] \end{aligned} \quad (6)$$

Considering the effects of repulsion and attraction on bacterial behaviour, the new fitness value of bacteria  $i$  after performing a chemotaxis operation is shown in the following formula (7):

$$J(i, j+1, k, l) = J(i, j, k, l) + J_{cc}(\theta^i(j+1, k, l)), P(j+1, k, l) \quad (7)$$

#### 2.4 Improvement of bacteria feeding algorithm

Bacteria will die out due to themselves and the environment when they are fed, and the disappearing bacteria will affect the number of populations and thus the accuracy of the algorithm. Therefore, in order to keep the bacterial population unchanged during the operation, a log-linear model is introduced into the bacterial population to ensure that the candidate feasible solutions of the algorithm will not change, as shown in formula (8):

$$P_r(t) = \frac{\left( \sum_m \exp[\beta_m h_m(t)] \right)}{\left( \sum_i \sum_m \exp[\beta_m h_m(t)] \right)} \quad (8)$$

Among them, the role of function  $h_m(t)$  ( $m = 1, 2, \dots, M$ ) is to improve the functional function of bacterial population diversity, as shown in formula (9):

$$h(t) = \frac{\sum_{i=1}^n |J(i, j, k, l) - J_{avg}^t|}{\left( N * \max_{1 \leq j \leq N} (|J(i, j, k, l) - J_{avg}^t|) \right)} \quad (9)$$

$h(t) \in (0, 1]$ .  $h(t) = 1$  means that the bacterial population diversity in the algorithm is poor, and the algorithm has few candidate feasible solutions. When  $h(t) < 1$ , the bacterial

population diversity in the algorithm is good. Among them, the  $J_{avg}^t$  function value represents the average fitness value of the bacterial population after completing  $t$  iterations, and  $J(i, j, k, l)$  represents the current fitness function value of the bacteria.

The trend and dispersal operations of the bacteria feeding algorithm are improved, and the inertia weight coefficient is added for the log-linear model, as shown in formula (10):

$$\omega_i = 0.6 * e^{(-\alpha * (1 - P_r(t)))} + 0.3 \quad (i = 1, 2, \dots, n) \quad (10)$$

Among them,  $\omega = [\omega_1, \omega_2, \dots, \omega_n]$  represents the inertia weight vector, and  $\omega_i (i = 1, 2, \dots, n)$  represents the inertia weight of the  $i^{\text{th}}$  dimension.  $\alpha$  is set to a constant 10, and the product is a dot product.

To optimise the tendency behaviour in the basic BFA according to the inertia weight, the bacteria update their position according to formula (11):

$$X_i^{t+1} = \frac{\omega_i X_i^t + (1 - \omega_i)(X_j^t - X_i^t)}{\|X_j^t - X_i^t\| \times \text{step} \times \text{rand}()} \quad (11)$$

Among them, the value of  $\text{rand}()$  takes any number in the closed interval  $[-1, 1]$ .

Bacteria can move according to formula (12) when performing dispersal behaviour:

$$X_i^{t+1} = \frac{\omega_i X_i^t + (1 - \omega_i)(X_{best}^t - X_i^t)}{\|X_{best}^t - X_i^t\| \times \text{step} \times \text{rand}()} \quad (12)$$

Among them,  $X_{best}$  is the optimal state of bacteria.

The following two formulas (13) and (14) can be used to adaptively adjust the value of the step size coefficient in the above problem:

$$C = C * \delta + C_{\min} \quad (13)$$

$$\delta = \exp(-3 \times (G/G_{\max})) \quad (14)$$

Among them,  $G$  and  $G_{\max}$  respectively represent the number of times the algorithm has executed dispersal and the maximum number of times to execute dispersal in the whole algorithm cycle. The product of formula (13) adopts dot product. The value of the step size  $C$  is larger in the initial stage of the algorithm, which can improve the efficiency of the algorithm and enable the algorithm to find the optimal value in a relatively short time in a large range. With the progress of the algorithm, the value of the step size  $C$  gradually decreases, which can improve the optimisation accuracy of the algorithm.

In order to maintain the diversity of the bacterial population after the bacteria perform the replication behaviour, the bacteria are mutated as in formula (15):

$$X_i' = X_i + X_i * N(0, 1) \quad (15)$$

Among them,  $N(0, 1)$  obeys the Gauss distribution with mean 0 and mean square error 1, and the product adopts dot product. Bacteria will automatically perform elimination and dispersal operation when they sense a high concentration of food, so that their individuals swim to the area. After the bacteria absorb the food nutrients in this area, the overall living environment of the bacteria changes (the food concentration is reduced, the pH is

unbalanced, the salinity is reduced, the water is reduced, etc.), and the bacterial viability is reduced, resulting in a decrease in the population. Therefore, in order to ensure the diversity of the bacterial population after the algorithm performs the elimination and dispersal operation, the Cauchy mutation shown in formula (16) is performed on the bacteria:

$$X_i' = X_i + X_i * C(0, 1) \quad (16)$$

Among them,  $C(0, 1)$  is the standard Cauchy distribution, and the product adopts the dot product.

### 3 Mathematical modelling of multi-UAV scenario planning based on 3D LiDAR

#### 3.1 Model building

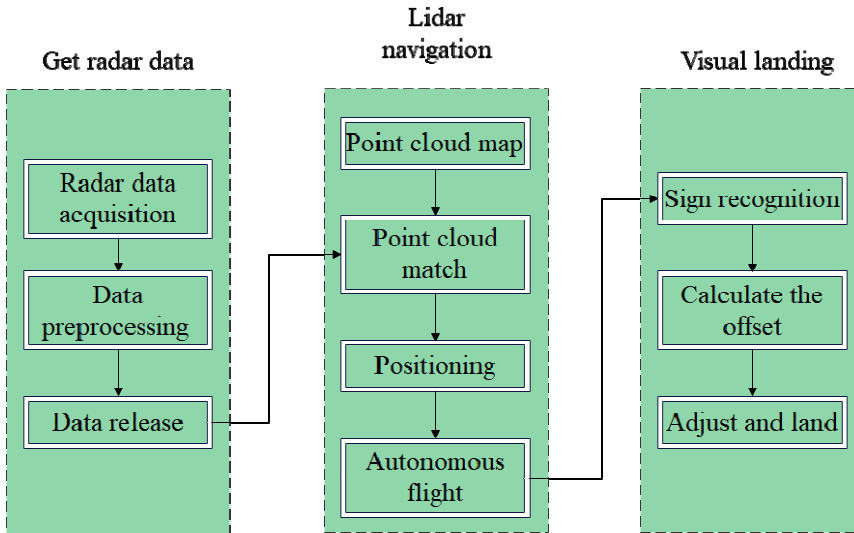
The traditional mathematical calculation methods, such as maximum likelihood method and trilateral measurement method, used in the classical algorithm are all a kind of estimation methods. When they are used, the difference between the final node estimated coordinates and the real coordinates will be too large, which will affect the final three-dimensional laser radar positioning and scanning effect. Considering this problem, we start with the intelligent optimisation algorithm, the traditional mathematical method is replaced by the bacterial foraging algorithm and Newton iteration method to calculate the corresponding subsequent node position coordinates. The specific steps are as follows:

- 1 Initialise the whole network. The specific steps are the same as those in the classical three-dimensional laser radar positioning and scanning algorithm. The beacon node of the wireless sensor network will generate information packets and forward them to its neighbour nodes within the communication radius. After receiving the packets, the node will transmit them to its neighbour nodes in the same way. The initial value of the hop value in the data packet is 0.
- 2 Calculate the minimum hop value between nodes and the average hop distance of beacon nodes. The specific steps are still the same as those in the classical three-dimensional laser radar location scanning algorithm. For the minimum hop value, unknown nodes will select the beacon node closest to themselves and retain the hop value between them. For average hop distance, the real distance between beacon nodes is calculated by GPS device, and then the average hop distance of beacon nodes can be obtained by dividing the real distance and hop value.
- 3 Calculate the estimated distance between beacon node and unknown node. The estimated distance between beacon node and unknown node can be obtained by multiplying the average hop distance and the minimum hop value in step 2.
- 4 The bacterial foraging algorithm is close to the unknown node coordinates, and the estimated distance between the beacon node and the unknown node in step 3 is substituted into the objective function. When the objective function value is the minimum, the coordinates obtained at this time are close to the real coordinates of the unknown node.

- Newton iteration method is accurate to the unknown nodes. The estimated coordinate data of the unknown nodes are calculated in step 4. However, due to the slow convergence speed of the bacteria foraging algorithm, the final results are not very accurate, and the accuracy of the solution of Newton iteration method will be affected by the initial value. Therefore, the results in step 4 are taken as the initial values of Newton iteration method to further refine the results.

In the second part, with the support of the multi-objective optimisation model based on bacteria algorithm, the mathematical modelling of multi-UAV scene planning based on 3D LiDAR is carried out, the 3D point cloud map is created, and the target point we are going to is set in the 3D point cloud map. Therefore, the positioning of the rotor UAV in the 3D point cloud map is very important. The positioning should not only mark the position of the UAV itself, but also make the error as small as possible. Then, go through the generated path to reach the specified destination point. Finally, the obstacles that appear during the movement are avoided, and the real-time problem of the rotor UAV is taken into account. Figure 5 shows the system function diagram.

**Figure 5** System function diagram (see online version for colours)



The design architecture is mainly distinguished by physical layer, protocol layer and application layer. The design architecture of the navigation system as shown in Figure 6 is given.

As shown in Figure 6, the UAV navigation architecture system enables real-time planning and scene analysis of the navigation process of the drone. It also enables real-time analysis of complex environments through sensors, analysing various hazardous factors and avoiding harmful factors in a timely manner.

The corresponding system hardware topology connection diagram is shown in Figure 7. It is divided into two modules, the UAV side and the ground station side, which correspond to each hardware in the physical layer.

**Figure 6** Design architecture of UAV navigation system (see online version for colours)

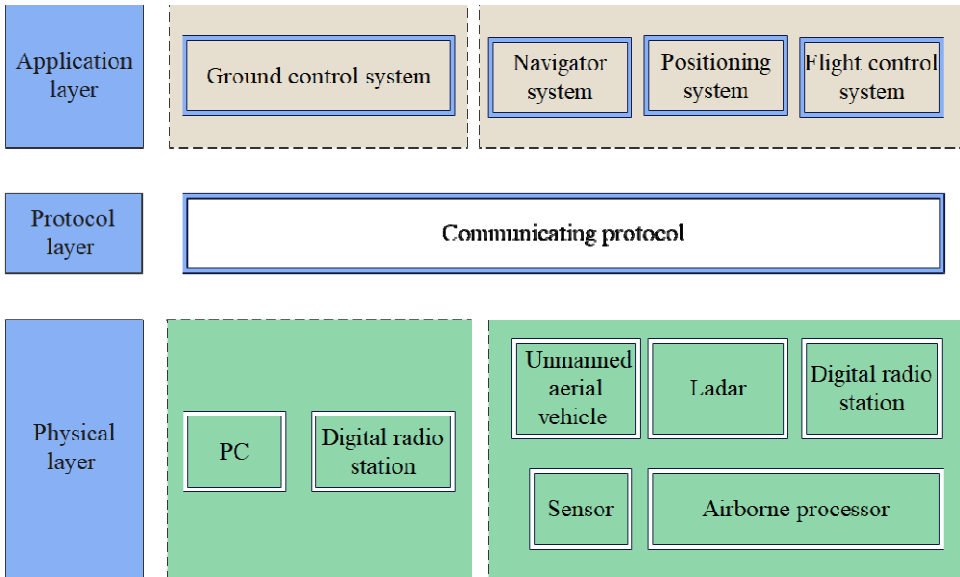
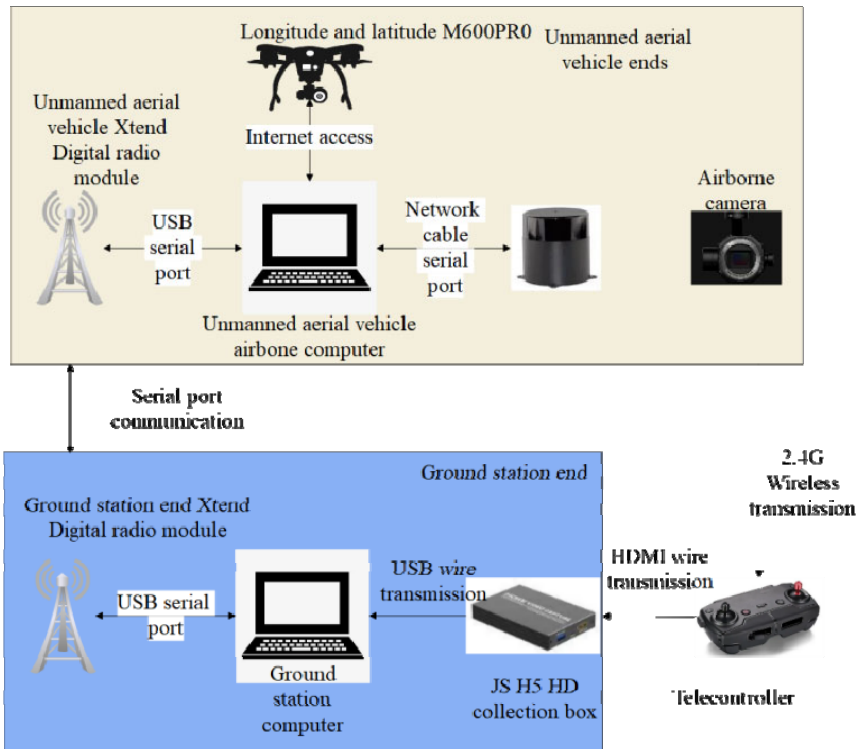
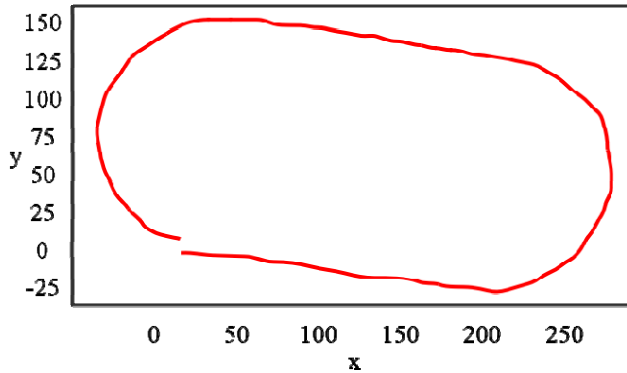


**Figure 7** Hardware topology of UAV navigation system (see online version for colours)



On the basis of the above model, the simulation test is carried out. There are obstacles such as power lines, flagpoles, and stands above the sports track, and adverse weather conditions were selected for experimental research. Figure 8 is the trajectory diagram of the manually controlled rotor UAV flying around the stadium runway. From the outline in the figure, it can be seen that the whole conforms to the flight trajectory, achieves the expected fusion positioning accuracy, and can meet the requirements of autonomous cruise.

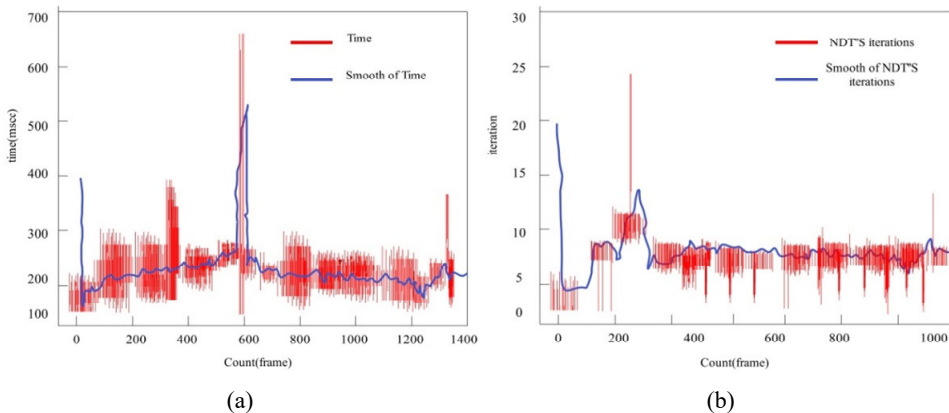
**Figure 8** Trajectory diagram (see online version for colours)



### 3.2 Results

Next, experimental research will be conducted on the planning and navigation processes of UAVs in various complex environments, and some data will be collected for intuitive display. The registration time of each frame of LiDAR data and the number of iterations of each frame of LiDAR data registration are sampled during the navigation process, as shown in Figure 9. The horizontal and vertical axes in the figure have corresponding descriptions. The red line is the original data, and the blue line is the smoothed data display.

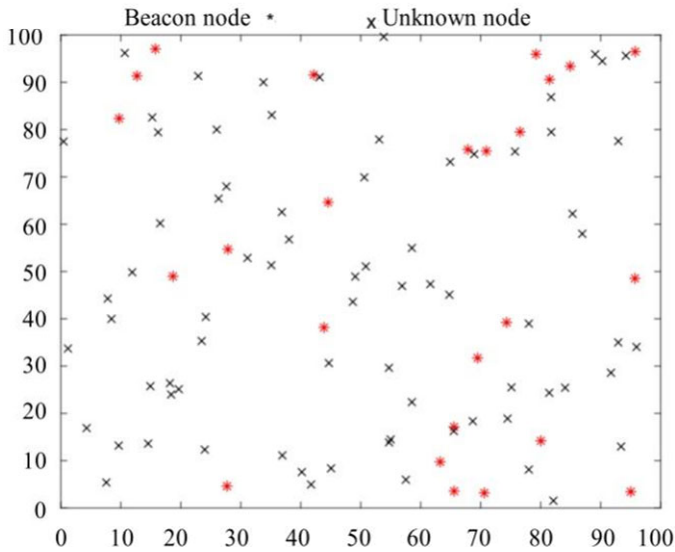
**Figure 9** 3D LiDAR navigation experiment, (a) registration time of laser points in navigation (b) number of iterations in navigation (see online version for colours)



Assume that the simulation experimental environment is a square two-dimensional area, randomly distribute wireless sensor nodes within it, and randomly select some wireless sensor nodes to load three-dimensional laser radar positioning devices as beacon nodes. The simulation experiment is carried out 50 times in each round, and the average value is taken as the final experimental result. The random deployment results of nodes are shown in Figure 10.

Compare the effectiveness of the drone scene planning model in this article with Choi et al. (2020), verify it through simulation platform, and compare it through manual evaluation. A total of 20 sets of comparisons were conducted, and the comparison results are shown in Table 1.

**Figure 10** The random deployment results of nodes (see online version for colours)



### 3.3 Analysis and discussion

When planning the trajectory of a drone, it is necessary to follow various constraints such as the drone's own characteristics, external environmental constraints, and task target constraints. If these constraints are not fully considered, the generated trajectory will not be able to reference flight. Therefore, it is necessary to consider various constraint information before the drone takes off, and plan a complete reference trajectory from the starting point to the target point according to the task requirements, that is, global static trajectory planning. However, currently, under typical complex environmental constraints, existing three-dimensional global static trajectory planning methods for UAVs have problems such as poor efficiency and low accuracy, and cannot balance the performance constraints of the drone itself. Therefore, this paper intends to conduct research on three-dimensional global static trajectory planning methods for UAVs that consider complex environmental constraints.

The drone trajectory planning algorithm supports and recognises digital information in the form of grid space. In the real trajectory planning area, there are many factors that affect the trajectory planning route, such as high-rise buildings, terrain peaks, various

dangerous elements, obstacles, task requirements, etc. These constraint information data sources are diverse and styles are different. If these factors are separately considered for their impact on trajectory planning, this will result in longer algorithm runtime and affect computational efficiency. Therefore, it is necessary to build an environmental model for UAV trajectory planning, which can not only effectively transform and integrate all factors that affect trajectory planning, but also directly provide grid digital information that the algorithm can recognise and process, facilitating algorithm search and calculation, thereby improving computational efficiency.

**Table 1** Comparative experimental results

<i>Number</i>	<i>The method of this article</i>	<i>The method of Choi et al. (2020)</i>
1	92.456	87.231
2	88.953	85.033
3	87.344	80.085
4	87.785	81.791
5	86.929	84.817
6	86.019	83.324
7	89.876	86.152
8	87.712	79.169
9	87.522	80.044
10	85.336	78.627
11	86.777	79.381
12	89.257	87.613
13	92.584	87.409
14	87.692	81.402
15	85.826	80.978
16	86.234	79.477
17	89.759	83.923
18	88.628	84.158
19	90.053	82.682
20	85.479	79.770

Due to the continuous movement of the radar coordinate system with the drone platform, obtaining complete information of the original three-dimensional scene in the world coordinate system requires unifying all the collected LiDAR data to the same coordinate system for fusion. Generally speaking, due to the high-frequency characteristics of radar sampling, the information collection of outdoor large-scale scenes usually includes thousands of frames of point cloud data, and there is a lack of overlapping scenes required for registration between distant point cloud data. Therefore, how to convert all point clouds to the same coordinate system based on registration information between adjacent frames is also an important issue that cannot be ignored in large-scale scene reconstruction.

After completing the fusion of point cloud frames, the originally sparse and uneven point clouds form point cloud blocks with relatively uniform resolution based on the first

frame of each group as the coordinate system. These point cloud blocks have similar amounts of data and a large number of overlapping areas, which can obtain more accurate results in registration calculations. After obtaining the coordinate transformation of point cloud blocks, if all spatial information is retained for the overlapping parts between point cloud blocks, it will cause a certain degree of data redundancy. Therefore, the simplification and smoothing of point cloud data in overlapping areas cannot be ignored.

This article studies the mathematical modelling of multi-drone scene planning, using 3D LiDAR technology as the basic navigation technology and bacterial foraging algorithm as the multi-objective optimisation algorithm. In order to address the shortcomings of the algorithm, appropriate improvements are made, and the bacterial population in the algorithm is introduced into the log-line model to improve the trend and migration of the algorithm, making the local search of the algorithm more accurate; Introducing Gaussian Cauchy mutation to ensure the diversity of bacterial population and ensure that the algorithm results are close to the global optimum. Combining the experimental research is to verify the model's effectiveness.

In Figure 9(a), when the UAV flies to an area with inconspicuous features, the longest registration time for fusion positioning is 731 ms. The smoothed curve is shown in the blue curve in the figure. Most of the registration time is 120 milliseconds on average, which meets the needs of real-time scene perception and poses estimation during cruise.

In Figure 9(b), the number of iterations exceeds the maximum number of iterations during the initial registration, and the registration is completed within the number of iterations in the rest of the time, and the average number of iterations is small. At the beginning of the registration, the initial pose is manually added on the ground station software, so it can quickly converge within the number of iterations.

As shown in Table 1, the evaluation results of drone scene planning in this paper are distributed in [88, 93], and the evaluation results of drone scene planning using the method proposed in Choi et al. (2020) are distributed in [78, 88], which verifies the feasibility of the proposed method.

From the above experimental research (Figure 10), it can be seen that the multi-UAV scene planning method based on 3D LiDAR can effectively improve the optimal control effect of multi-UAVs and improve the working efficiency of UAV swarms.

## 4 Conclusions

LiDAR is a new type of measurement technology that has developed rapidly in the past decade. It emits a single-band laser beam and obtains the three-dimensional coordinate information of surface objects according to the echo of the ground objects, thereby generating point clouds to realise the extraction of ground object information and the reconstruction of three-dimensional scenes. Due to its high angular resolution and strong anti-interference ability, it has been widely used in research fields such as remote sensing data detection, ground model restoration and reconstruction, and has great application prospects. This paper studies the mathematical modelling of multi-UAV scene planning, and uses 3D LiDAR as the basis to verify the model effect through intelligent simulation. The experimental study shows that the multi-UAV scene planning method based on 3D LiDAR can effectively improve the optimal control effect of multi-UAV.

The research in this article is based on computer simulation systems, and attempts can be made to implement the enhanced synthetic visual scheme designed in this article on

embedded platforms, striving to move towards real application scenarios. The feasibility of the proposed model can be further verified in practice.

## References

- Baca, T., Petrlik, M., Vrba, M., Spurny, V., Penicka, R., Hert, D. and Saska, M. (2021) 'The MRS UAV system: pushing the frontiers of reproducible research, real-world deployment, and education with autonomous unmanned aerial vehicles', *Journal of Intelligent & Robotic Systems*, Vol. 102, No. 1, pp.1–28.
- Basiri, A., Mariani, V., Silano, G., Aatif, M., Iannelli, L. and Glielmo, L. (2022) 'A survey on the application of path-planning algorithms for multi-rotor UAVs in precision agriculture', *The Journal of Navigation*, Vol. 75, No. 2, pp.364–383.
- Batinovic, A., Petrovic, T., Ivanovic, A., Petric, F. and Bogdan, S. (2021) 'A multi-resolution frontier-based planner for autonomous 3D exploration', *IEEE Robotics and Automation Letters*, Vol. 6, No. 3, pp.4528–4535.
- Choi, Y., Chen, M., Choi, Y., Briceno, S. and Mavris, D. (2020) 'Multi-UAV trajectory optimization utilizing a NURBS-based terrain model for an aerial imaging mission', *Journal of Intelligent & Robotic Systems*, Vol. 97, No. 1, pp.141–154.
- Choi, Y.J., Ramatryana, I.N.A. and Shin, S.Y. (2021) 'Cellular communication-based autonomous UAV navigation with obstacle avoidance for unknown indoor environments', *International Journal of Intelligent Engineering and Systems*, Vol. 14, No. 2, pp.344–352.
- Hongming, S.H.E.N., Qun, Z.O.N.G., Hanchen, L.U., Zhang, X., Bailing, T.I.A.N. and Lei, H.E. (2022) 'A distributed approach for LiDAR-based relative state estimation of multi-UAV in GPS-denied environments', *Chinese Journal of Aeronautics*, Vol. 35, No. 1, pp.59–69.
- Krátký, V., Petráček, P., Báča, T. and Saska, M. (2021) 'An autonomous unmanned aerial vehicle system for fast exploration of large complex indoor environments', *Journal of Field Robotics*, Vol. 38, No. 8, pp.1036–1058.
- Le, T., Gjevestad, J.G.O. and From, P.J. (2019) 'Online 3D mapping and localization system for agricultural robots', *IFAC-PapersOnLine*, Vol. 52, No. 30, pp.167–172.
- Miao, Y., Tang, Y., Alzahrani, B.A., Barnawi, A., Alafif, T. and Hu, L. (2020) 'Airborne LiDAR assisted obstacle recognition and intrusion detection towards unmanned aerial vehicle: architecture, modeling and evaluation', *IEEE Transactions on Intelligent Transportation Systems*, Vol. 22, No. 7, pp.4531–4540.
- Petráček, P., Krátký, V., Petrlik, M., Báča, T., Kratochvíl, R. and Saska, M. (2021) 'Large-scale exploration of cave environments by unmanned aerial vehicles', *IEEE Robotics and Automation Letters*, Vol. 6, No. 4, pp.7596–7603.
- Petrlik, M., Báča, T., Heřt, D., Vrba, M., Krajník, T. and Saska, M. (2020) 'A robust UAV system for operations in a constrained environment', *IEEE Robotics and Automation Letters*, Vol. 5, No. 2, pp.2169–2176.
- Qin, H., Meng, Z., Meng, W., Chen, X., Sun, H., Lin, F. and Ang, M.H. (2019) 'Autonomous exploration and mapping system using heterogeneous UAVs and UGVs in GPS-denied environments', *IEEE Transactions on Vehicular Technology*, Vol. 68, No. 2, pp.1339–1350.
- Quan, L., Han, L., Zhou, B., Shen, S. and Gao, F. (2020) 'Survey of UAV motion planning', *IET Cyber-systems and Robotics*, Vol. 2, No. 1, pp.14–21.
- Selecký, M., Faigl, J. and Rollo, M. (2019) 'Analysis of using mixed reality simulations for incremental development of multi-UAV systems', *Journal of Intelligent & Robotic Systems*, Vol. 95, No. 1, pp.211–227.
- Șmuleac, A., Herbei, M., Popescu, G., Popescu, T., Popescu, C.A., Barliba, C. and Șmuleac, L. (2019) '3D modeling of patrimonium objectives using laser technology, Bulletin of University of Agricultural Sciences and Veterinary Medicine Cluj-Napoca', *Horticulture*, Vol. 76, No. 1, pp.106–113.

- Tang, Y., Hu, Y., Cui, J., Liao, F., Lao, M., Lin, F. and Teo, R.S. (2018) ‘Vision-aided multi-UAV autonomous flocking in GPS-denied environment’, *IEEE Transactions on Industrial Electronics*, Vol. 66, No. 1, pp.616–626.
- Ulku, E.E., Dogan, B., Demir, O. and Bekmezci, I. (2019) ‘Sharing location information in multi-UAV systems by common channel multi-token circulation method in FANETs’, *Elektronika ir Elektrotechnika*, Vol. 25, No. 1, pp.66–71.
- Wang, D., Fan, T., Han, T. and Pan, J. (2020) ‘A two-stage reinforcement learning approach for multi-UAV collision avoidance under imperfect sensing’, *IEEE Robotics and Automation Letters*, Vol. 5, No. 2, pp.3098–3105.
- Zhou, X., Yi, Z., Liu, Y., Huang, K. and Huang, H. (2020) ‘Survey on path and view planning for UAVs’, *Virtual Reality & Intelligent Hardware*, Vol. 2, No. 1, pp.56–69.
- Zohdi, T. (2020) ‘The game of drones: rapid agent-based machine-learning models for multi-UAV path planning’, *Computational Mechanics*, Vol. 65, No. 1, pp.217–228.